coatings

MDPI

Article

Influence of Surface Nanocrystallization on Two-Step Pack-Boronizing of AISI 5120 Steel

Xinyu Zhang [1], Na Tian [1,*], Baojian Liu [1], Zhanwei Yuan [2], Runze Zhao [1] and Liling Ge [1]

[1] School of Materials Science and Engineering, Xi'an University of Technology, Xi'an 710048, China; zhangxinyu1@xaut.edu.cn (X.Z.); liubaojian@xaut.edu.cn (B.L.); 3200111028@stu.xaut.edu.cn (R.Z.); geliling-xut@163.com (L.G.)
[2] School of Materials Science and Engineering, Chang'an University, Xi'an 710061, China; yuanyekingfly@163.com
* Correspondence: tianna@xaut.edu.cn

Abstract: AISI 5120 steel, which underwent 30 min single-surface nanocrystallization via supersonic fine particle bombarding (SFPB), was pre-boronized at 600 °C for 2 h, and then final-boronized at 800 °C or 900 °C for 2–6 h, i.e., two-step pack-boronizing. The specimens' microstructure and mechanical characteristics before and after two-step boronizing were examined in detail. The results showed that the hardness of the SFPB surface reached 570 HV, which was 2.73 times higher than its original hardness (209 HV). The nanocrystallized surface exhibited the increased thickness and hardness of the boride layer, in comparison to that of the un-SFPB surface. Two-step pack-boronizing further improved the thickness and hardness of the SFPB surface of AISI 5120 steel. When final-boronizing at 900 °C for 6 h, the thickness and hardness of the boronizing layer in the SFPB surface was 88 μm and 2196 HV, respectively, which was 10.5 times higher than the original hardness. Additionally, the CeO_2 added in the boronizing agent was helpful in obtaining the boride layer with the ductile-serrated Fe_2B phase rather than the brittle phase of FeB in the boride layer, which was expected for industrial applications.

Keywords: AISI 5120; surface nanocrystallization; two-step pack-boronizing

check for updates

Citation: Zhang, X.; Tian, N.; Liu, B.; Yuan, Z.; Zhao, R.; Ge, L. Influence of Surface Nanocrystallization on Two-Step Pack-Boronizing of AISI 5120 Steel. *Coatings* **2023**, *13*, 1242. https://doi.org/10.3390/coatings13071242

Academic Editor: Roberto Montanari

Received: 31 May 2023
Revised: 5 July 2023
Accepted: 8 July 2023
Published: 13 July 2023

Copyright: © 2023 by the authors. Licensee MDPI, Basel, Switzerland. This article is an open access article distributed under the terms and conditions of the Creative Commons Attribution (CC BY) license (https://creativecommons.org/licenses/by/4.0/).

1. Introduction

Boronizing is one of the best methods for the acquisition of a highly wear-resistant surface for metallic components. The boride layer possesses high hardness, good abrasion resistance, and excellent oxidation resistance [1–3]. This process is easy to implement using relatively simple equipment, and includes pack-boronizing, liquid-boronizing, and gas-boronizing, etc. [3–5]. Among the conventional boronizing methods, pack-boronizing, with its low cost, is popularly used, because there is no need for special equipment, the component does not need to be cleaned after boronizing, the boronizing agent can be reused, and the depth and microstructure of the boride layer can be easily controlled [6–9]. However, traditional boronizing is performed at high temperatures, ranging from 850 °C to 1050 °C, for a long time (3–16 h), which results in the deformation of the component and high energy consumption. These demerits mentioned above limit its application. Therefore, it is becoming a popular topic to reduce the temperature and accelerate the boronizing rate.

It has been reported that surface nanocrystallization cannot only improve the surface strength, wear resistance, and fatigue resistance of bulk materials, but can also improve the chemical reaction activity, so as to reduce the temperature of the surface chemical heat treatment [10,11]. Using the surface mechanical attrition treatment, surface nanocrystallization was carried out on samples of EN8 steel, and then the nanocrystallized samples were boronized via pack-boronizing [12]. It was found that the surface mechanical attrition treatment of EN8 steel samples could be boronized using a desired case depth at 650 °C for 7 h, which was much lower than the conventional boronizing temperature. A

similar process was also performed for AISI 304 stainless steel [13]. The surface-mechanical-attrition-treated AISI 304 stainless steel was pack-boronized via single-stage (at 950 °C for 1, 3, 5, and 7 h) and duplex (700 °C for 1 h and 950 °C for 1 h) treatments. It was reported that the surface mechanical attrition treatment increased the kinetics of boron diffusion in AISI 304 stainless steel, enabled the formation of a higher volume fraction of alloy borides, and increased the hardness of the boride layer in the steel. The duplex treatment obviously increased the case depth in the sample more than the single-step treatment did. A nanostructured surface layer was also fabricated on H13 steel using air blast shot peening [14]. By means of a duplex boronizing treatment at T_1 = 600 °C for 2 h, followed by T_2 = 850 °C for 8 h, the thicknesses of the Fe_2B phase in the air blast shot peening sample and the coarse-grained counterpart were 40 μm and 30 μm, respectively. The above reports indicate that surface nanocrystallization could be used as a pre-treatment for the boronizing of steel, which would not only greatly reduce the temperature of the chemical heat treatment and shorten the boronizing time, but would also provide necessary precautions for boron concentration to control the volume fraction of the deleterious FeB phase. Therefore, surface crystallization is of great significance to realize low energy consumption, low pollution, and the controllable nitriding of a product in chemical heat treatment.

In this work, surface nanocrystallization was carried out using supersonic fine particle bombarding (SFPB) [15,16], which is suitable for complex shapes and large-area metal components. The disk of AISI 5120 steel, one of the most commonly used steels in engineering, was nanocrystallized on one side of the sample for 30 min, while the other side was maintained in its original state. Then, the samples were subjected to pack-boronizing at 600 °C for 2 h using the agent with an appropriate amount of CeO_2, followed by heating to 800 °C and 900 °C for 2, 4, and 6 h, respectively, for two-step pack-boronizing. At the same time, single-step boronizing with the same boronizing agent was also performed for SFPBed samples, by directly heating to 900 °C for 4 h, as the control group. The effects of the boronizing temperature and time under two various processes and conditions on the microstructure and mechanical properties of the boronized layer are discussed in detail. Especially, the two-step pack-boronizing process for AISI 5120 steel was optimized, and the boronizing behavior of this specimen was systematically investigated, aiming to provide an effective approach for the practical application of surface nanocrystallization in engineering materials.

2. Experimental Procedures

AISI 5120 steel was selected, whose chemical composition (wt.%) is shown as follows: C: 0.21; Cr: 0.97; Mn: 0.66; Si: 0.18; S: no more than 0.03; P: no more than 0.03; Fe: balance. The steel bar was annealed at 950 °C for 2 h and then cut into disks with diameters of 60 mm and thicknesses of 4 mm.

Only one surface of the steel disk was surface nanocrystallized, while the other surface maintained its original state. The bombardment process could be described as follows: the working pressure was 0.55 MPa, the diameter of the S110 stainless steel shot was 0.3 mm, and the processing duration was 30 min. After SFPB, the specimens were boronized via two-step pack-boronizing, first at 600 °C for 2 h, and then they were heated up to 800 °C or 900 °C for 2, 4, and 6 h. The boronizing agent powder consisted of B_4C, Na_2SiF_6, CeO_2, C, and SiC. Na_2SiF_6 was used as the activation agent of the boronizing agent. The boronizing sealing tank and the agent were dried at 100 °C for 1 h. Then, the sample with the boronizing agent powder was sealed up in the tank. The boronizing treatment was carried out in a muffle furnace. Finally, the sealed tank was cooled in the air.

The microstructure and phase constitution of the boronized AISI 5120 steel samples were characterized using an Olympus microscope (GX-71), X-ray diffractometer (XRD-7000S), and high-resolution transmission electron microscopy (TEM, JEM-3010). The microhardness of the AISI 5120 steel samples was measured using a nano-Indenter (G200) with 50 gf for 10 s. The composition of the boronizing layer was checked via energy dispersive spectrometry (EDS), (Oxford X-MaxN type).

3. Results and Discussion

3.1. Microstructure and Hardness of Sample after SFPB

Figure 1 depicts the cross-sectional microstructure of the annealed AISI 5120 steel sample treated via SFPB and the hardness profile along the depth of the deformed layer. The deformation layer in the AISI 5120 steel sample after the SFPB was noticeably distinct from the matrix, since the initial grains in the annealed state were relatively coarse (approximately 20~50 μm) (see Figure 1a). After the SFPB, the depth of the deformation layer was about 220 μm, in which the depth of the severe deformation layer was about 35 μm. The change trend in the hardness value with depth is shown in Figure 1b. It can be seen that the hardness dramatically declined from the surface to a depth of 50 μm, and that the ferrite and pearlite structures could not be distinguished at this site, which was part of a heavily deformed layer. The hardness gradually declined from the surface to the matrix in the depth range of 50 to 225 μm. The surface hardness of 570 HV was 2.73 times the original matrix hardness of 209 HV.

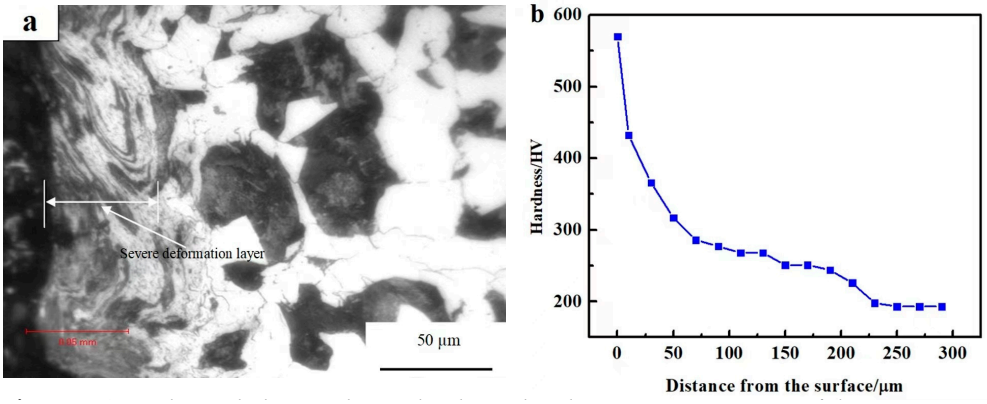


Figure 1. Optical morphology and microhardness distribution in cross-section of the SFPB-treated AISI 5120 steel sample: (**a**) optical morphology; (**b**) microhardness distribution from surface to interior.

Figure 2 shows the XRD patterns of the surface layer of the AISI 5120 steel sample that were exposed to the SFPB for 30 min, where the diffraction peaks corresponded to ferrite and its average grain size was around 19.4 nm, determined using the Scherrer–Wilson formula. Figure 3 gives the bright and dark transmission electron microscope images and the corresponding selected area electron diffraction (SAED) patterns obtained at the site 10 μm from the surface of the SFPB AISI 5120 steel sample. The SAED patterns were indexed as the ferrite. Its average grain size in the surface was also about 19 nm, indicating that the grains in the surface were refined to the nanometer scale after the SFPB treatment.

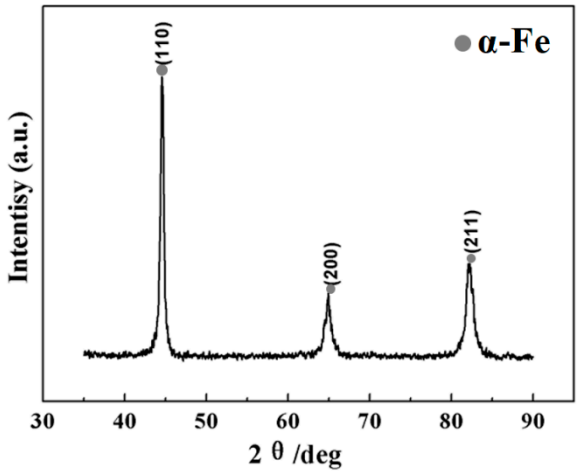


Figure 2. X-ray diffraction patterns of SFPB AISI 5120 steel sample after SFPB for 30 min.

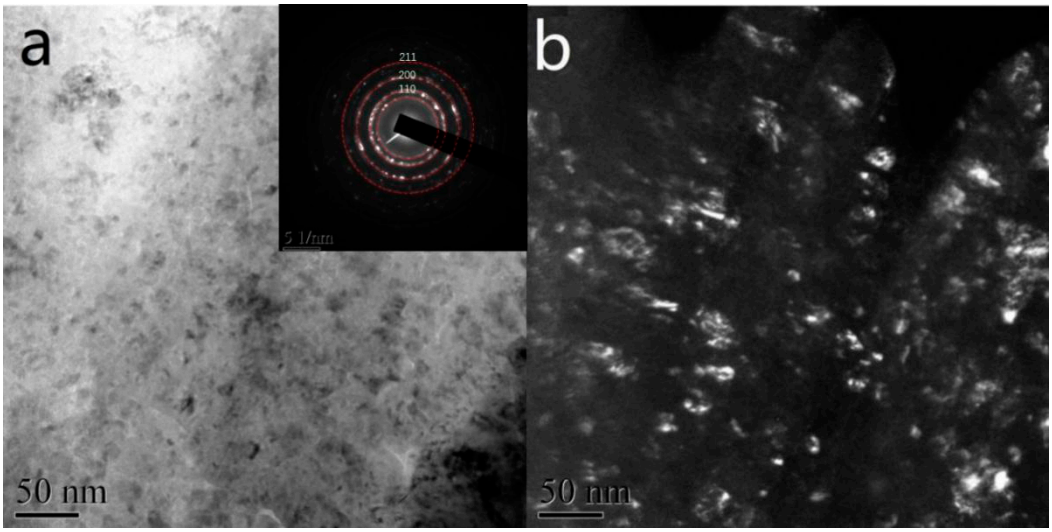


Figure 3. TEM images and corresponding SAED patterns obtained at the site 10 μm from the surface of the SFPB AISI 5120 steel side: (**a**) bright field image and corresponding SAED pattern insets; (**b**) dark field image.

3.2. Characteristics of the Boride Layer for SFPB and Un-SFPB Surfaces

The cross-sectional microstructures of the boronized AISI 5120 steel samples are shown in Figure 4. The boride layer was not observed in both the SFPB and un-SFPB surfaces after pre-boronizing at 600 °C for 2 h (as seen in Figure 4a,b), while the obvious deformation layer in the SFPB surface can still be observed in Figure 4a. This indicates that recrystallization did not occur in the surface deformation layer during pre-boronizing. The boride layers were observed in the SFPB surface and the un-SFPB surface when second-step boronizing was carried out at 800 °C for 2 h (as seen in Figure 4c,d). The thickness of the boride layer in the SFPB surface was about 20 μm, as seen in Figure 4c. The boride with a finger shape was inserted into the matrix, but the interface of the boride layer and substrate was not very clear. The amount of pearlite between the boride layer and the substrate increased, and the grains of pearlite and ferrite were obviously refined, forming a transition region with a depth of about 50 μm. However, the depth of the boride layer in the un-SFPB surface was about 17 μm in Figure 4d, and the boundary between the boride layer and the substrate was well-defined. Although the amount of pearlite also increased between the boride layer and the substrate, the grains were not as fine as the grains in the SFPB surface. When the boronizing temperature increased to 900 °C, the boron diffusion coefficient and activity increased. Combined with the effect of pre-boronization at 600 °C for 2 h and the increase in B concentration in the surface, the driving force for the boride layer formation also increased. The thicknesses of the boride layers for both the SFPB and the un-SFPB surfaces obtained at 900 °C were much larger than those obtained at 800 °C (Figure 4e,f). The thickness of the boride layer was about 65 μm in the SFPB side and the jagged boride morphology was very clear, which was vertically inserted into the matrix, resulting in a firm joint between the boride layer and the matrix. At the same time, the boride layer also possessed a very high density and could protect the matrix for a long time. However, the thickness of the boride layer in the un-SFPB AISI 5120 steel side was about 57 μm.

The microstructures of the boride layer in the SFPB and the un-SFPB surfaces of AISI 5120 steel samples boronized at 900 °C for 4 and 6 h are shown in Figure 5. It can be seen that the thickness of the boronizing layer obtained at 900 °C for 4 h was about 71 μm in the SFPB surface (as seen in Figure 5a) and approximately 60 μm in the un-SFPB surface (as seen in Figure 5b). When boronizing for 6 h, the thickness of the boride layer reached about 88 μm in the SFPB surface (as seen in Figure 5c), where the boride with the shape of sharp fingertips was gained and countercrossed with the matrix very well, to avoid the

boride layer spalling. But, the thickness of the boride layer in the un-SFPB surface is about 68 µm (as seen in Figure 5d).

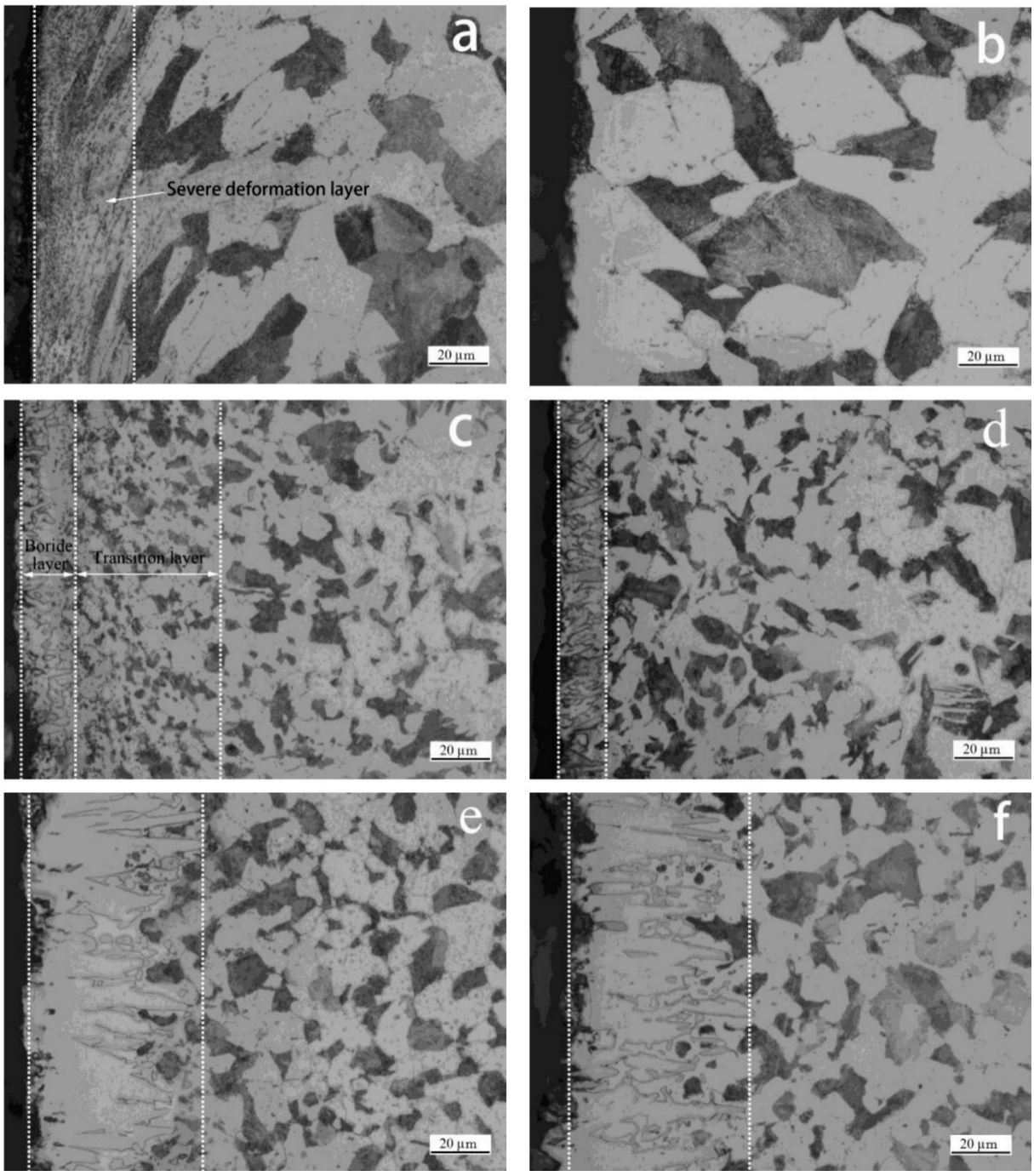


Figure 4. Cross-sectional microstructure of the different boronized AISI 5120 steel samples: (**a**) boronized at 600 °C for 2 h of SFPB surface and (**b**) boronized at 600 °C for 2 h of un-SFPB surface; (**c**) second-step boronizing at 800 °C for 2 h of SFPB surface and (**d**) second-step boronizing at 800 °C for 2 h of un-SFPB surface; (**e**) second-step boronizing at 900 °C for 2 h of SFPB surface and (**f**) second-step boronizing at 900 °C for 2 h of un-SFPB surface.

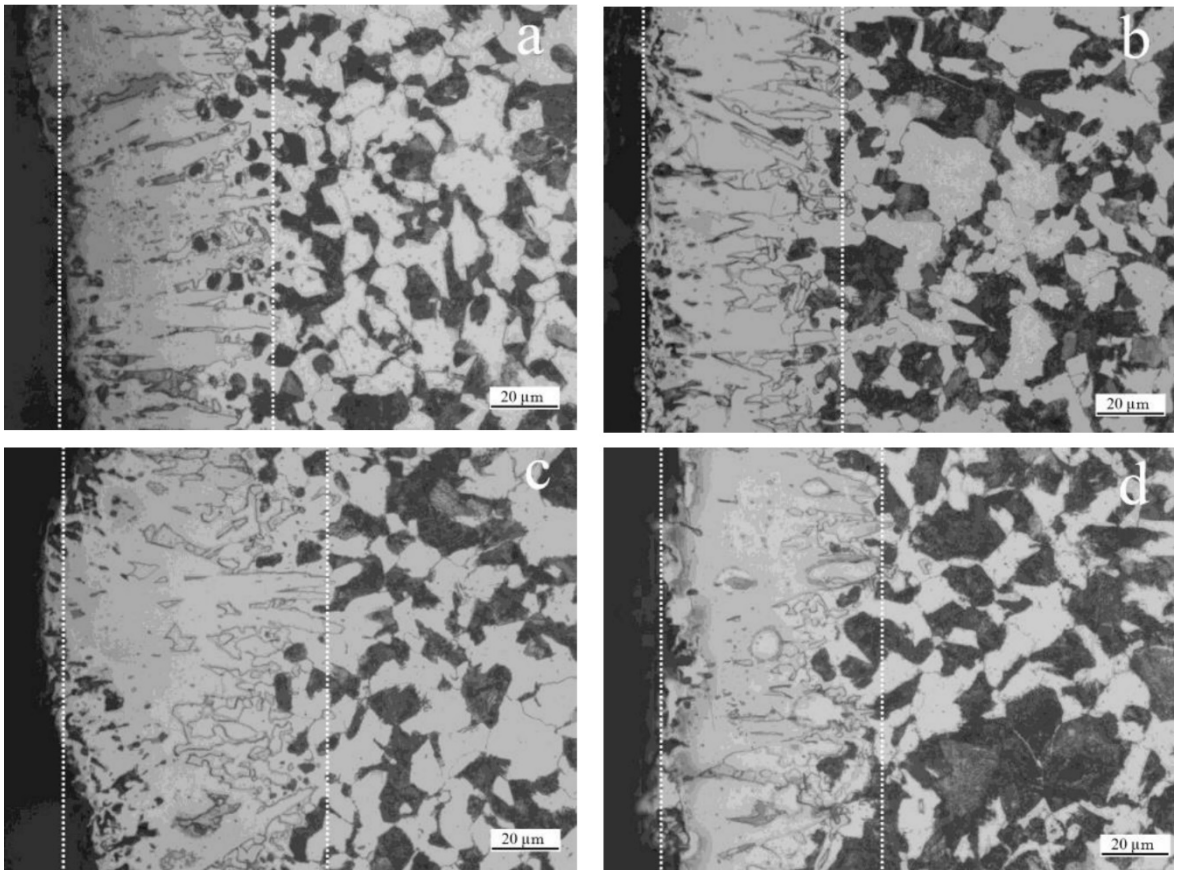


Figure 5. Cross-sectional microstructure of the different boronized AISI 5120 steel samples after second-step boronizing at 900 °C for (**a**) 2 h with SFPB, (**b**) 2 h with un-SFPB, (**c**) 4 h with SFPB, and (**d**) 4 h with un-SFPB.

The relationship between the boride depths in the SFPB and the un-SFPB surfaces of the AISI 5120 steel samples and the boronizing temperature and time are shown in Figure 6. It can be seen that the thickness of the boride layer continually increased with the extension of the boronizing temperature or time. However, the boride layer thickness in the SFPB surface increased faster than that in the un-SFPB surface.

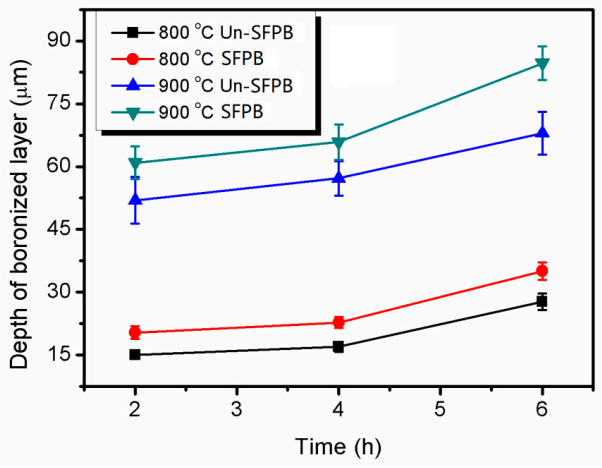


Figure 6. The depths of the boride layer in SFPB and un-SFPB surfaces of AISI 5120 steel samples with varying boronizing temperature and time.

3.3. Phase Constituents and Hardness of Boride Layer

Figure 7 gives the XRD patterns for the SFPB AISI 5120 steel sample after pre-boronizing at 600 °C for 2 h followed by second-step boronizing at 900 °C for 6 h. It can be seen that a single Fe_2B phase existed in the boride layer after boronizing. The SEM image after the microhardness test and the hardness profile of the SFPB and un-SFPB AISI 5120 steel samples are shown in Figures 8 and 9, which were boronized at 600 °C for 2 h followed by boronizing at 900 °C for 2 h and 6 h, respectively. For the SFPB sample boronized at 900 °C for 2 h, the hardness at the site with a depth of 20 μm from the surface was about 1898 HV. Its hardness gradient was moderate, and the thickness of the diffusion layer was 40 μm. As for the un-SFPB surface after the same boronizing process, the hardness at a similar depth from the surface was 1606 HV. It exhibited a steep gradient in the boride layer and the thickness of the diffusion layer was about 20 μm. When the boronizing time was prolonged to 6 h, the hardness at the site with a depth of 20 μm from the surface was about 2196 HV. The thickness of the boride layer increased significantly (about 60 μm). The thickness of the diffusion layer increased to 60 μm, and the hardness gradient was flatter. Compared with the SFPB surface, the thickness of the boride layer for the un-SFPB surface was small (about 40 μm, as seen in Figure 8b). The thickness of the diffusion layer in the un-SFPB surface was about 30 μm, and the hardness gradient was steeper.

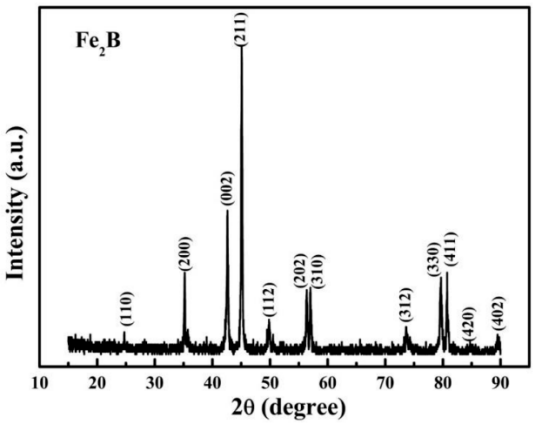


Figure 7. XRD pattern for the SFPB AISI 5120 steel sample after pre-boronizing at 600 °C for 2 h combined with second-step boronizing at 900 °C for 6 h.

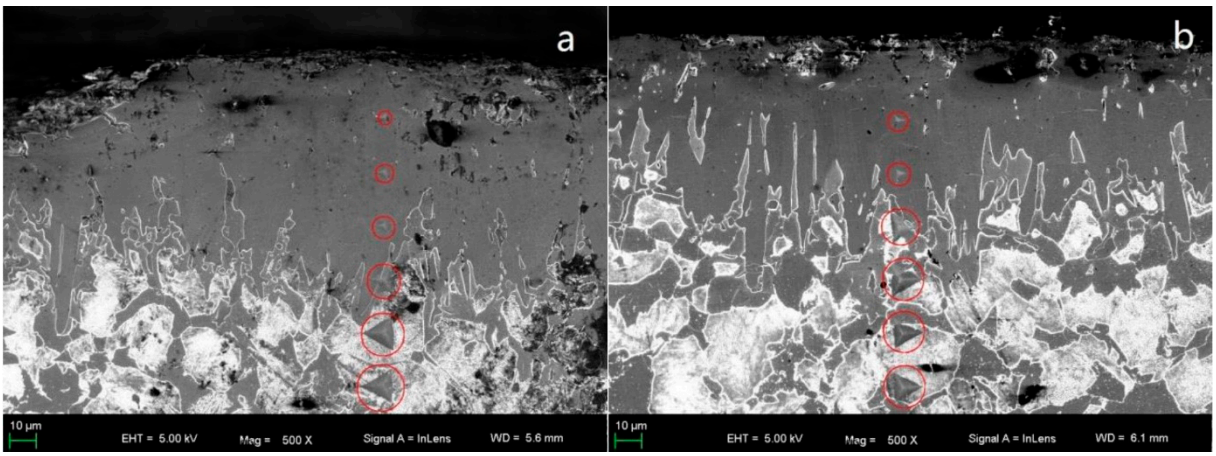


Figure 8. SEM image after microhardness test experiment of AISI 5120 steel samples with (**a**) second-step boronizing at 900 °C for 2 h of SFPB surface and (**b**) un-SFPB surface.

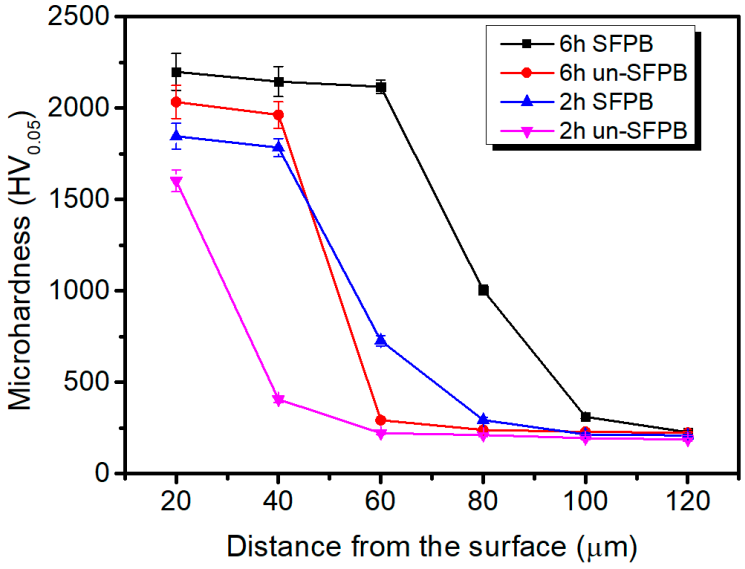


Figure 9. Hardness profile of the SFPB and un-SFPB surfaces of AISI 5120 steel samples, boronized at 600 °C for 2 h combined with second-step boronizing at 900 °C for 2 h and 6 h, respectively.

Figure 10 shows the selected area composition in the SFPB surface of AISI 5120 steel samples after pre-boronizing at 600 °C for 2 h combined with second-step boronizing at 900 °C for 2 h (a) and 6 h (b). It was found that the main elements in the samples were Fe, Cr, Ce, and B. There was an obvious difference in the elemental distribution at different positions. In Figure 10a, area A corresponded to the boride with 11.88 wt.% B, 1.09 wt.% Cr, 87.02 wt.% Fe, and 0.01 wt.% Ce. Area B corresponded to the non-boride zone with 11.88 wt.% B, 0.59 wt.% Cr, 99.37 wt.% Fe, and 0.02 wt.% Ce, while B was not detected in this position. A similar phenomenon can be seen in Figure 10b. It was found that the Cr was enriched in the boride layer (in area A and area C), while the non-boride zone was depleted of such an element (in area B and area D) after two-step pack-boronizing. Cr could partially replace Fe to form alloyed Fe_2B, which could increase the hardness of the sample [17]. The distribution of Ce was opposite to the distribution of Cr, which suggested that it was hard for Ce to exist in the borides, and Ce diffused from the surface to the matrix. The explanation for this phenomenon is not inconsistent at present. It was believed that although the atomic radius of rare Earth elements is large, the polarization between rare Earth elements and typical non-metallic elements could inevitably lead to a reduction in their ionic radius [18]. Therefore, Ce that cannot enter the boride diffused into the interior of the sample. Further investigation is also expected on this topic.

When the second-step boronizing time increased from 2 h (Figure 10a) to 6 h (Figure 10b), a denser and thicker boride layer formed in the surface of the sample. It could be interpreted that the longer time helped to generate the Fe_2B phase during the incubation period, which caused the deep and large area cross-linking [19].

3.4. Formation Mechanism of the Boride Layer

There were a large number of grain boundaries and dislocations in the surface of the AISI 5120 specimen after the SFPB treatment, which can provide lots of channels for boron atom diffusion. The traditional boronizing temperature was in the range of 850 °C to 1050 °C. The grain in the surface could grow due to the high treatment temperature, and then the diffusion channel decreased, resulting in the limitation of the B atom diffusion. Although the borides did not form during boronizing at 600 °C for 2 h, there were large volume fractions of the deformation area, as well as grain boundaries and defects (as seen in Figure 4a), which were helpful for boron atoms to diffuse into the surface of the specimen, resulting in the high concentration of the boron atom in the surface. This can effectively enhance the driving force of second-step high-temperature boronizing [12,13]. Therefore,

with the increase in the boronizing temperature, the boride layer thickness increased and the increment for the SFPB surface was much larger than that for the un-SFPB surface (as seen in Figure 4c–f). Especially in the SFPB surface, a thick finger-shaped boride layer (about 20 μm) formed at 800 °C. The boride layer and the substrate had a good joint. The amount of pearlite between the boronizing layer and the substrate increased, and the grains of pearlite and ferrite were obviously refined, forming a transition region with the depth of about 50 μm (as seen in Figure 4c).

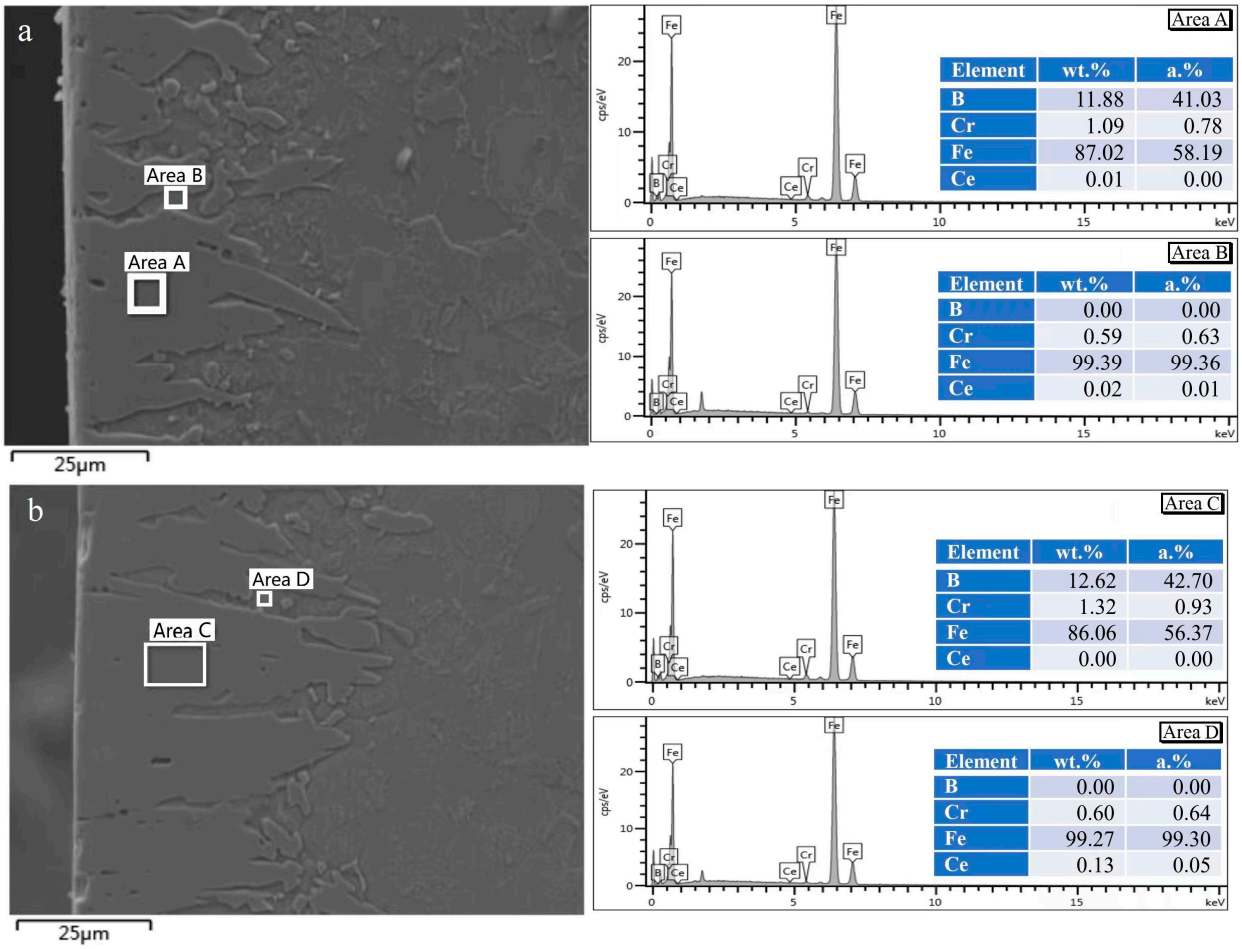


Figure 10. Area composition analysis for AISI 5120 steel samples with second-step boronizing at 900 °C for (**a**) 2 h and (**b**) 6 h.

The process of boride formation could be summarized as follows: (1) With the boride formation during the boronizing process for AISI 5120 steel, carbon and alloy elements in steels (Cr and Mn) were squeezed to the deeper channel along these defects. A transition zone enriched the carbon and alloying elements could form between the boride layer and the matrix, so as to increase the amount of pearlite in this zone. (2) The content of the pearlite increased and the pearlite was refined due to the air cooling after boronizing. (3) CeO_2 added in the boronization agent made the boride fine and the amount of the phase between the fingers decrease. But, when the temperature reached 900 °C, the increase in the diffusion coefficient and activity of boron enhanced the driving force for the formation of boride and the thickness of the boride layer (as seen in Figure 4e,f). A similar phenomenon occurred when the boronizing time was prolonged (as seen in Figures 5 and 6).

The flow diagram of the two-step pack-boronizing process of AISI 5120 steel is shown in Figure 11. The surface nanocrystallization of AISI 5120 steel via SFPB increased the volume fractions of grain boundary and crystal defects in the surface. On the one hand, this provided more opportunities for the nucleation of iron boride, which was helpful to obtain

the fine iron and boron phase. On the other hand, CeO_2 added in the boronization agent acted as a catalyst, which could not only refine the grains in the boride layer, but could also increase the concentration of vacancy defects in the steel surface. Additionally, CeO_2 could accelerate the decomposition, absorption, and diffusion of boronization agents. This made the formation of the brittle phase of FeB difficult due to the relatively low concentration of the B atom, while it was easy to obtain the single Fe_2B phase. Therefore, the single Fe_2B phase was found when boronizing at the high temperature of 900 °C for 6 h. The increase in the Fe_2B phase amount in the boride layer could enhance the hardness of the SFPB surface and widen the depth of the boride layer, resulting in a good hardness gradient (Figures 8 and 9). The improvement of the microhardness of the boride layer could also be attributed to the effect of alloying elements and rare Earth elements. It was reported that alloying elements in steel, such as Cr, Mn, and Mo, can improve the hardness of the boride layer, without an obvious inhibiting effect on the growth of borides. There was 0.97 wt.% Cr and 0.66 wt.% Mn in AISI 5120 steel. The Cr atom existed as the substitutional atom in Fe_2B, which not only increased the hardness of the boride layer but also changed the valence electron structure of Fe_2B. Especially when the content of Cr is 0.5 wt. %, Cr can significantly improve the fracture toughness of the Fe_2B phase [20]. Ce and Fe also form displacement solid solutions, which can cause crystal lattice distortion and increase the hardness of the boride layer.

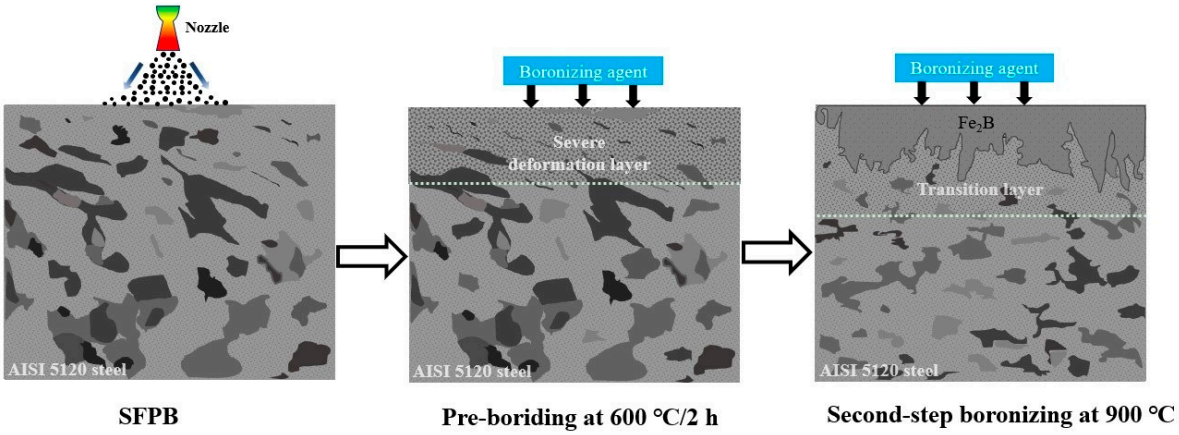


Figure 11. The sketch of SFPB with two-step boronizing for AISI 5120 steel samples.

4. Conclusions

The single surfaces of AISI 5120 steel disks were nanocrystallized via SFPB. The disks were boronized via the two-step boronizing process with the agent adding the appropriate amount of CeO_2. In the pre-boronizing process at 600 °C, there were still large amounts of grain boundary and dislocation defects, which provided lots of diffusion channels for B atoms, resulting in an enhancement in the driving force of second-step high-temperature boronizing. Therefore, it was easier to obtain a deeper and denser boride layer with higher hardness and a flatter hardness gradient for the SFPB surface than the un-SFPB surface, which indicated that surface nanocrystallization can be used as an effective pre-treatment for the boronizing of AISI 5120 steel. In addition, surface nanocrystallization and the addition of CeO_2 also promoted obtaining the single ductile Fe_2B phase, while the formation of the brittle FeB phase was suppressed in the boride layer.

Author Contributions: Investigation, X.Z.; writing—review and editing, N.T., B.L. and Z.Y.; methodology, R.Z.; supervision, L.G. All authors have read and agreed to the published version of the manuscript.

Funding: This work was in part supported by the National Natural Science Foundation of China (no. 52171191), the International Science and Technology Cooperation Program of Shaanxi Key R&D Program (no. 2021KWZ-12), and the China Postdoctoral Science Foundation (no. 2017M623084).

Institutional Review Board Statement: Not applicable.

Informed Consent Statement: Not applicable.

Data Availability Statement: The data presented in this study are available upon reasonable request from the authors.

Conflicts of Interest: All authors declare no conflict of interest.

References

1. Campos-Silva, I.; Ortiz-Dominguez, M.; Lopez-Perrusquia, N.; Meneses-Amador, A.; Escobar-Galindo, R.; Martinez-Trinidad, J. Characterization of AISI 4140 borided steels. *Appl. Surf. Sci.* **2010**, *256*, 2372–2379. [CrossRef]
2. Turkmen, I.; Yalamac, E. Growth of the Fe_2B layer on sae 1020 steel employed a boron source of H_3BO_3 during the powder-pack boriding method. *J. Alloy. Compd.* **2018**, *744*, 658–666. [CrossRef]
3. Kul, M.; Danac, I.; Gezer, S.; Karaca, B. Effect of boronizing composition on hardness of boronized AISI 1045 steel. *Mater. Lett.* **2020**, *279*, 128510. [CrossRef]
4. Özsoy, A.; Yaman, Y.M. The effect of thermocycling liquid boronizing on the thickness of the boride layer and the transition zone. *Scr. Metall. Mater.* **1993**, *29*, 231–236. [CrossRef]
5. Kartal, G.; Timur, S.; Sista, V.; Eryilmaz, O.L.; Erdemir, A. The growth of single Fe_2B phase on low carbon steel via phase homogenization in electrochemical boriding (PHEB). *Surf. Coat. Technol.* **2011**, *206*, 2005–2011. [CrossRef]
6. Cimenoglu, H.; Atar, E.; Motallebzadeh, A. High temperature tribological behaviour of borided surfaces based on the phase structure of the boride layer. *Wear* **2014**, *309*, 152–158. [CrossRef]
7. Sarma, B.; Chandran, K.S.R. Accelerated kinetics of surface hardening by diffusion near phase transition temperature: Mechanism of growth of boride layers on titanium. *Acta Mater.* **2011**, *59*, 4216–4228. [CrossRef]
8. Kartal, G.; Timur, S.; Eryilmaz, O.L.; Erdemir, A. Influence of process duration on structure and chemistry of borided low carbon steel. *Surf. Coat. Technol.* **2010**, *205*, 1578–1583. [CrossRef]
9. Taktak, S. Some mechanical properties of borided AISI H13 and 304 steels. *Mater. Des.* **2007**, *28*, 1836–1843. [CrossRef]
10. Lu, K.; Lu, J. Surface nanocrystallization (SNC) of metallic materials-presentation of the concept behind a new approach. *J. Mater. Sci. Technol.* **1999**, *15*, 193–197.
11. Pogrebnjak, A.; Ivashchenko, V.; Bondar, O.; Beresnev, V.; Sobol, O.; Załęski, K.; Jurga, S.; Coy, E.; Konarski, P.; Postolnyi, B. Multilayered vacuum-arc nanocomposite TiN/ZrN coatings before and after annealing: Structure, properties, first-principles calculations. *Mater. Charact.* **2017**, *134*, 55–63. [CrossRef]
12. Balusamy, T.; Narayanan, T.S.N.S.; Ravichandran, K. Effect of surface mechanical attrition treatment (Smat) on boronizing of en8 steel. *Surf. Coatings Technol.* **2012**, *213*, 221–228. [CrossRef]
13. Balusamy, T.; Narayanan, T.S.N.S.; Ravichandran, K.; Park, I.S.; Min, H.L. Effect of surface mechanical attrition treatment (Smat) on pack boronizing of aisi 304 stainless steel. *Surf. Coatings Technol.* **2013**, *232*, 60–67. [CrossRef]
14. Yang, H.; Wu, X.; Cao, G.; Yang, Z. Enhanced boronizing kinetics and high temperature wear resistance of H13 steel with boriding treatment assisted by air blast shot peening. *Surf. Coatings Technol.* **2016**, *307*, 506–516. [CrossRef]
15. Zhang, Y.X.; Yang, J.H.; Ge, L.L.; Zhang, X.; Chen, J.Z. Research on mechanism of surface nanocrystalline layer in 2219 Al alloy induced by supersonic fine particles bombarding. *Int. J. Eng. Res. Afr.* **2016**, *24*, 1–8.
16. Ge, L.L.; Tian, N.; Lu, Z.X.; You, C.Y. Influence of the surface nanocrystallization on the gas nitriding of Ti-6Al-4V alloy. *Appl. Surf. Sci.* **2013**, *286*, 412–416.
17. Mei, S.; Zhang, Y.; Zheng, Q.; Fan, Y.; Lygdenov, B.; Guryev, A. Compound boronizing and its kinetics analysis for H13 steel with rare earth CeO_2 and Cr_2O_3. *Appl. Sci.* **2022**, *12*, 3636. [CrossRef]
18. Cheng, X.; Xie, C. Study on the Mechanism of Rare Earth Elements in Chemical Heat Treatment of Steel. *J. Chin. Rare Eart.* **1994**, *12*, 336–339.
19. Keddam, M.; Kulka, M.; Makuch, N.; Pertek, A.; Małdziński, L. A kinetic model for estimating the boron activation energies in the FeB and Fe_2B layers during the gas-boriding of armco iron: Effect of boride incubation times. *Appl. Surf. Sci.* **2014**, *298*, 155–163. [CrossRef]
20. Ma, R.N.; Fan, Y.Z.; Cao, X.M.; Wen, M. Influence of micro-addition chromium on the valence electron structure and toughness of Fe_2B phase. *Appl. Mech. Mater.* **2010**, *34*, 1135–1139.

Disclaimer/Publisher's Note: The statements, opinions and data contained in all publications are solely those of the individual author(s) and contributor(s) and not of MDPI and/or the editor(s). MDPI and/or the editor(s) disclaim responsibility for any injury to people or property resulting from any ideas, methods, instructions or products referred to in the content.